THE JOURNAL OF PHYSICAL CHEMISTRY Letters

Letter

pubs.acs.org/JPCL

# Why Is Cobalt the Best Transition Metal in Transition-Metal Hangman Corroles for O−O Bond Formation during Water Oxidation?

Wenzhen Lai,*[,†] Rui Cao,*[,†] Geng Dong,[†] Sason Shaik,[§] Jiannian Yao,[‡] and Hui Chen*[,‡]

[†]Department of Chemistry, Renmin University of China, Beijing 100872, China

[‡]Beijing National Laboratory of Photochemistry, Institute of Chemistry, Chinese Academy of Sciences, Beijing 100190, China

[§]Institute of Chemistry and the Lise Meitner-Minerva Center for Computational Quantum Chemistry, The Hebrew University of Jerusalem, Givat Ram Campus, 91904 Jerusalem, Israel

Supporting Information

**ABSTRACT:** O−O bond formation catalyzed by a variety of β-octafluoro hangman corrole metal complexes was investigated using density functional theory methods. Five transition metal elements, Co, Fe, Mn, Ru, and Ir, that are known to lead to water oxidation were examined. Our calculations clearly show that the formal $Co^{V}$ catalyst has a $Co^{IV}$−corrole$^{\bullet+}$ character and is the most efficient water oxidant among all eight transition-metal complexes. The O−O bond formation barriers were found to change in the following order: Co(V) ≪ Fe(V) < Mn(V) < Ir(V) < Co(IV) < Ru(V) < Ir(IV) < Mn(IV). The efficiency of water oxidation is discussed by analysis of the O−O bond formation step. Thus, the global trend is determined by the ability of the ligand d-block to accept two electrons from the nascent $OH^{-}$, as well as by the $OH^{\bullet}$ affinity of the TM(IV)═O species of the corresponding TM(V)═O·$H_2O$ complex. Exchange-enhanced reactivity (EER) is responsible for the high catalytic activity of the Co(V) species in its $S$ = 1 state.

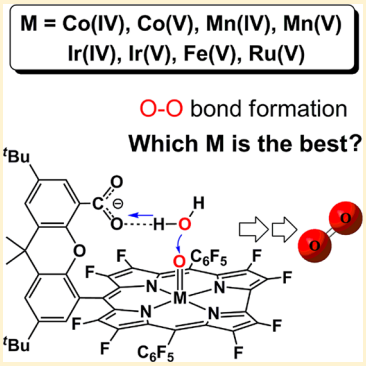


**SECTION:** Molecular Structure, Quantum Chemistry, and General Theory

Water oxidation is a crucial process in artificial photosynthesis, which constitutes an attractive way to use solar energy and convert it to chemical forms.[1−5] Thus, an $O_2$ molecule is released by extracting four electrons and four protons. This process is neither thermodynamically nor kinetically favorable, and consequently, it requires efficient catalysis. In addition to nanostructured metal oxides and well-characterized multinuclear metal complexes which serve as competent water oxidation catalysts (WOCs), recent advances have been made in the use of single transition-metal (TM) complexes as water oxidants.[5−14] These latter active complexes mainly include Ru, Ir, Mn, Fe, and Co. The accepted mechanism of $O_2$ generation, catalyzed by a single TM site, involves O−O bond formation via a base-assisted nucleophilic attack of a $H_2O$ molecule on a high-valent TM-oxo, as for example, in Scheme 1.[5,15−17] This mechanism has been supported by several theoretical studies.[10−12,17−26]

Scheme 1 shows the cobalt hangman β-octafluoro corrole (Cor) WOC that was recently made by Nocera and co-workers.[27] On the basis of the pH dependence of the oxygen-evolving reaction catalyzed by this complex, a proton-coupled electron-transfer (PCET) mechanism was suggested. A Co(V) species has been postulated as the active catalytic species for water oxidation. In addition, the exact electronic structure of the proposed precatalyst, the Co(IV) species, as either Co(IV)−Cor or Co(III)−Cor$^{\bullet+}$, remains unclear. In order to assign the reactive oxidation state and the mechanistic details, we used density functional theory (DFT) to explore the

**Scheme 1. Co Hangman Corrole Complex**

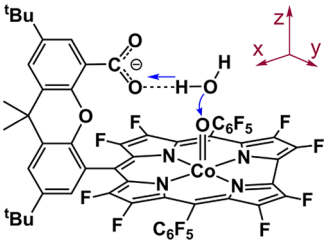

detailed O−O bond formation pathways (see Scheme 1) nascent from Co hangman corrole complexes with two possible high-valent cobalt-oxo species, formally Co(IV) and Co(V). Furthermore, our study addresses a key question, whether or not cobalt is the optimal TM for water oxidation in such a hangman corrole environment. To these ends, we systematically examined the O−O bond formation process for a variety of TMs that are known to be active for water oxidation and determined the effect of their oxidation states on the process. We thus studied the following high-valent TMs: Co(IV), Co(V), Mn(IV), Mn(V), Fe(V), Ru(V), Ir(IV), and Ir(V). Here, the labeled oxidation state of the metal is just the formal oxidation number without counting the possible electron

**Received:** June 30, 2012
**Accepted:** August 5, 2012
**Published:** August 6, 2012



   dx.doi.org/10.1021/jz3008535 | J. Phys. Chem. Lett. 2012, 3, 2315−2319

**Table 1. All Barrier Heights, Reaction Energies, and the Electronic Configurations for the RC and PC in the Most Favorable Pathway for Each System**

| TM | reaction barrier[a] $\Delta G^{\ddagger}$ (kcal/mol) | reaction energy[a] $\Delta G$ (kcal/mol) | electronic configuration | |
|---|---|---|---|---|
| | | | RC | PC |
| Co(IV) | 29.1 ($^2$TS-$^2$RC) | 24.0 ($^2$PC-$^2$RC) | $^2$RC: $(d_{xy})^2(\pi^*_{yz})^2(\pi^*_{xz})^1(\sigma^*_{z^2})^0(\phi_{cor})^2$ | $^2$PC: $(d_{xy})^2(\pi^*_{yz})^2(\pi^*_{xz})^2(\sigma^*_{z^2})^1(\phi_{cor})^2$ |
| Co(V) | 3.6 ($^3$TS-$^3$RC) | −8.8 ($^1$PC-$^3$RC) | $^3$RC: $(d_{xy})^2(\pi^*_{yz})^2(\pi^*_{xz})^1(\sigma^*_{z^2})^0(\phi_{cor})^1$ | $^1$PC: $(d_{xy})^2(\pi^*_{yz})^2(\pi^*_{xz})^2(\sigma^*_{z^2})^0(\phi_{cor})^2$ |
| Mn(IV) | 58.3 ($^4$TS-$^4$RC) | 55.1 ($^4$PC-$^4$RC) | $^4$RC: $(d_{xy})^1(\pi^*_{yz})^1(\pi^*_{xz})^1(\sigma^*_{z^2})^0(\phi_{cor})^2$ | $^4$PC: $(d_{xy})^2(\pi^*_{yz})^1(\pi^*_{xz})^1(\sigma^*_{z^2})^1(\phi_{cor})^2$ |
| Mn(V) | 20.5 ($^5$TS-$^1$RC) | 6.3 ($^5$PC-$^1$RC) | $^1$RC: $(d_{xy})^2(\pi^*_{yz})^0(\pi^*_{xz})^0(\sigma^*_{z^2})^0(\phi_{cor})^2$ | $^5$PC: $(d_{xy})^1(\pi^*_{yz})^1(\pi^*_{xz})^1(\sigma^*_{z^2})^1(\phi_{cor})^2$ |
| Fe(V) | 18.5 ($^2$TS-$^4$RC) | 4.2 ($^4$PC-$^4$RC) | $^4$RC: $(d_{xy})^2(\pi^*_{yz})^1(\pi^*_{xz})^1(\sigma^*_{z^2})^1(\phi_{cor})^1$ | $^4$PC: $(d_{xy})^2(\pi^*_{yz})^1(\pi^*_{xz})^1(\sigma^*_{z^2})^1(\phi_{cor})^0$ |
| Ru(V)[b] | 35.1 ($^2$TS-$^2$RC) | 34.5 ($^2$PC-$^2$RC) | $^2$RC: $(d_{xy})^2(\pi^*_{yz})^1(\pi^*_{xz})^0(\sigma^*_{z^2})^0(\phi_{cor})^2$ | $^2$PC: $(d_{xy})^2(\pi^*_{yz})^2(\pi^*_{xz})^1(\sigma^*_{z^2})^0(\phi_{cor})^2$ |
| Ir(IV) | 52.5 ($^2$TS-$^2$RC) | 52.1 ($^2$PC-$^2$RC) | $^2$RC: $(d_{xy})^2(\pi^*_{yz})^2(\pi^*_{xz})^1(\sigma^*_{z^2})^0(\phi_{cor})^2$ | $^2$PC: $(d_{xy})^2(\pi^*_{yz})^2(\pi^*_{xz})^2(\sigma^*_{z^2})^1(\phi_{cor})^2$ |
| Ir(V) | 23.0 ($^1$TS-$^3$RC) | 21.7 ($^1$PC-$^3$RC) | $^3$RC: $(d_{xy})^2(\pi^*_{yz})^1(\pi^*_{xz})^1(\sigma^*_{z^2})^0(\phi_{cor})^2$ | $^1$PC: $(d_{xy})^2(\pi^*_{yz})^2(\pi^*_{xz})^2(\sigma^*_{z^2})^0(\phi_{cor})^2$ |

[a]The two corresponding spin states (denoted with the superscript) involved in the free-energy difference measurement are labeled in parentheses; a negative reaction energy means an exothermic reaction. [b]For TM = Ru(V), data are calculated from the PBE0/B2 level because the B3LYP functional fails to generate TS and PC on a very flat potential energy surface.

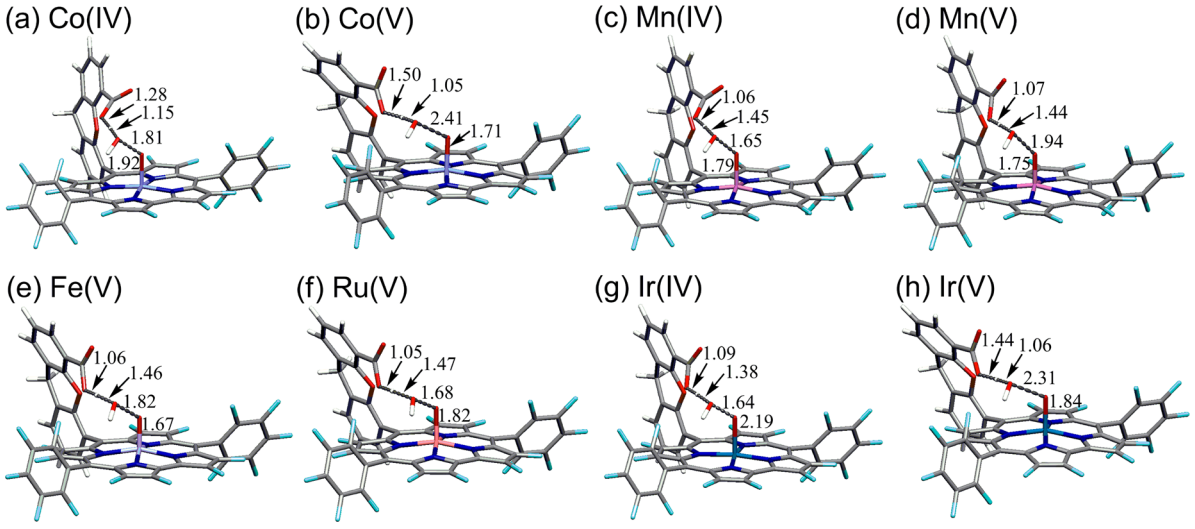


**Figure 1.** All TS geometries in the most favorable pathway for the O−O bond formation process.

transfer from the corrole ring to lead to a noninnocent corrole ligand. Unless stated otherwise, all reported computational energetics below are the free energies from B3LYP/def2-TZVP/CPCM (denoted as B3LYP/B2) based on geometries optimized with B3LYP/def-SV/CPCM in water (denoted as B3LYP/B1). The computational details are relegated to the Supporting Information (SI). As shown in the SI (Table S1), the conclusions of this work are almost not dependent on the identity of the functional used. Below, we focus on the key computational results.

To assess the energetic accessibility of high-valent TM(V)═O species, we calculated the redox potentials for the TM(IV)═O/TM(V)═O couple, which are 1.07, 0.91, 1.12, 0.43, and 0.34 V versus NHE for Co−, Mn−, Fe−, Ru−, and Ir−hangman corrole complexes, respectively. As such, all high-valent TM(V)═O species included in this work are accessible. In addition, all of the corresponding TM corrole complexes are known in the literature;[9,28,29] therefore, our computational study is associated with experimentally designed systems. As such, this timely comparative study aims for a better understanding of the factors controlling mononuclear TM-catalyzed water oxidation. Moreover, the study establishes the impact of these TMs and their different oxidation states on the O−O bond formation. As shall be seen, the trends follow a clear physical principle, which may be helpful toward the design of new competent WOCs.

The first issue concerns the Co−hangman corrole complex responsible for the O−O bond formation step; is it Co(IV) or Co(V)?[27] To answer this question, we studied the O−O bond formation process with both possible oxidation states. First, we explored the reactant clusters (RCs) of the complexes with $H_2O$, which are $[(H^{\beta F}CX{-}CO_2)Co(IV){=}O{\cdot}H_2O]^{2-}$ and $[(H^{\beta F}CX{-}CO_2)Co(V){=}O{\cdot}H_2O]^{-}$ species. The Co(IV) RC has a doublet spin ground state ($S$ = 1/2). The corresponding quartet ($S$ = 3/2) state is degenerate with the doublet, only 0.01 kcal/mol higher in energy at the B3LYP/B2 level. Both doublet and quartet states of the Co(IV) RC have metal-oxo-centered unpaired electrons and bear no corrole ring radicaloid. Thus, the experimentally proposed precatalytic state of the Co hangman corrole species, $[(H^{\beta F}CX{-}CO_2)Co(IV){=}O]^{2-}$, is best described as Co(IV)−Cor rather than Co(III)−Cor$^{\bullet+}$. In contrast to the Co(IV)−Cor RC, the lowest-lying Co(V) RC species involves a corrole ring cation radicaloid character, thus having a Co(IV)−Cor$^{\bullet+}$ electronic configuration. The lowest electronic states of the formal Co(V) RC involve therefore two virtually degenerate singlet ($S$ = 0) and triplet ($S$ = 1) states due to the weak interaction between the $S$ = 1/2 Cor$^{\bullet+}$ and the $S$ = 1/2 Co(IV)═O center. The $S$ = 1 state results from a


dx.doi.org/10.1021/jz3008535 | J. Phys. Chem. Lett. 2012, 3, 2315−2319

ferromagnetic coupling, while the $S$ = 0 state involves antiferromagnetic coupling. The $S$ = 1 state is 0.7 kcal/mol lower in energy than the $S$ = 0 state. The quintet ($S$ = 2) state of the Co(V) RC, which has a quartet Co(IV)═O center ferromagnetically coupled to the corrole ring radicaloid, is 1.9 kcal/mol higher than the $S$ = 1 ground state.

The lowest transition states (TSs) for O−O formation in Co(IV) and Co(V) are, respectively, on the doublet and triplet potential energy surfaces. For Co(IV), the quartet TS is slightly higher in energy than the doublet state by 0.1 kcal/mol. As shown in Table 1, the lowest O−O bond formation TSs of Co(IV) and Co(V) species lie, respectively, 29.1 and 3.6 kcal/mol higher than the corresponding lowest RCs. The experimental activation barrier for water oxidation in this Co hangman corrole system is 17.6 kcal/mol (the turnover frequency = 0.81 $s^{-1}$).[27] Hence, Co(IV) has too high of a barrier to be able to act as catalyst, while Co(V), that is, Co(IV)−Cor$^{\bullet+}$, is the active catalytic state, as proposed by Nocera and co-workers. Meanwhile, Co(IV)−Cor$^{\bullet+}$ has a much lower O−O bond formation barrier than the experimental value, suggesting that the O−O bond formation step is not the rate-determining step in such a system. In addition, consistent with the Hammond postulate,[30] the Co(V) TS ($R_{O-O}$ = 2.41 Å) is much earlier than the Co(IV) TS ($R_{O-O}$ = 1.81 Å), as shown in Figure 1a and b.

Interestingly, although the $S$ = 0 and 1 Co(V) RCs are almost degenerate (the $S$ = 1 product (PC) is 1.2 kcal/mol higher than the $S$ = 0 one), still the $S$ = 1 TS is 10.1 kcal/mol lower than the singlet one. This may be in discord with the Bell−Evans−Polanyi (BEP)[31,32] principle, which states that a thermodynamically advantaged process should have a lower TS energy. Thus, the Co(V)-mediated O−O formation could be another example where spin states make a difference in reactivity.[33−36] The electron rearrangements during the O−O bond formation for Co(V) singlet and triplet states are depicted in Scheme 2. It can be seen that during the O−O bond formation reactions, the number of unpaired electrons on Co increases from one to two for the triplet state but decreases from one to zero for the singlet state. Therefore, while the triplet TS is stabilized by a new exchange interaction, the singlet TS is not. As such, the triplet reaction is typified by exchange-enhanced reactivity (EER),[35,36] which lowers the barriers in reactions that exhibit an increase of the number of unpaired electrons on the TM center in the TS. In addition, it is seen that the O−O distance of the triplet TS ($R_{O-O}$ = 2.41 Å) is much earlier than that of the singlet TS ($R_{O-O}$ = 2.05 Å). Thus, here, we witness a Hammond effect in the absence of the BEP effect. Contrary to the Co(V) species, the EER was not observed for the Co(IV) species because the number of unpaired electrons remains unchanged during the O−O bond formation, and the reaction thermodynamics of the nucleophilic attack is poor, as expected from the lower electrophilicity of Co(IV)-oxo.

**Scheme 2. Orbital Occupancy Evolution during O−O Bond Formation in the (a) Singlet and (b) Triplet States of the Co(V) System**

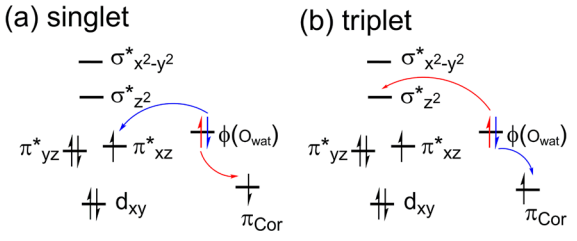


How do other TMs and their related oxidation states affect the O−O bond formation reaction? Table 1 summarized our computed lowest O−O bond formation barriers for a variety of TM-containing hangman corrole species, together with the electronic configuration of the lowest RC and PC. It should be noted that besides Co(V)═O, the Fe(V)═O species also has a corrole ring cation radicaloid character, while others do not. The corresponding TS geometries are shown in Figure 1. From Table 1, we can see that among all of these cases, Co(V) has by far the lowest O−O bond formation barrier, and the order of calculated barriers is Co(V) < Fe(V) < Mn(V) < Ir(V) < Co(IV) < Ru(V) < Ir(IV) < Mn(IV). Thus, our calculations demonstrate that Co(V) in the $S$ = 1 state is the best for catalyzing the O−O bond formation process among the TM-containing hangman corrole complexes. As such, the experimental finding of catalytic effectiveness of Co in the hangman corrole complex for water oxidation is corroborated theoretically. In general, for all studied TM-containing hangman corrole systems, the species with a formal oxidation number of V is more reactive than its corresponding one with a formal oxidation number of IV in the O−O bond formation reactions, which is consistent with the nucleophile (water)−electrophile (TM═O) character of this reaction.

As shown in Figure 1, the analysis of the forming O−O bond distances of all TSs indicates that for TMs within the same subfamily, like Fe and Ru or Co and Ir, the barriers vary in the opposite order to O−O bond distances, which means that the smaller the O−O bond distance, the higher the barrier height. As such, within the same subfamily, the Hammond postulate is observed. Notably in Table 1, there are three cases, Fe(V), Mn(V), and Ir(V), in which the spin state identity from the lowest RC to the lowest TS changes. This indicates that spin crossover must be involved in the O−O bond formation steps. For these three systems, the gaps to promote the RC from its lowest spin state (quartet/singlet/triplet) to the lowest spin state of the TS (doublet/quintet/singlet) are small (1.0/2.7/6.0 kcal/mol, respectively) and may lead to spin pre-equilibrium.

The reaction energies of all reactions are also shown in Table 1. Interestingly, we can see that the global trend in the barriers is dominated by the reaction energies, which vary in the order Co(V) < Fe(V) < Mn(V) < Ir(V) < Co(IV) < Ru(V) < Ir(IV) < Mn(IV). Therefore, as far as metal identity is concerned, the BEP principle is followed. The reaction energy order of the O−O bond formation step involves nucleophilic attack of the nascent $OH^-$ on the TM═O center (Scheme 1), and consequently, the d-block is enriched by two electrons. Our calculations show that the reaction energy ordering within the 3d TM complex is controlled by the ease of the two-electron reduction of the TM═O center (Table S4, SI). Thus, moving from left to right in the 3d period, the two-electron reduction becomes easier. Consequently, the reaction energy becomes more exothermic (less endothermic) in the order Co(V) > Fe(V) > Mn(V), therefore leading to a higher reactivity in the same order. By contrast, going down a family in the TMs, for example, from Co(V) to Ir(V) and from Fe(V) to Ru(V), the relative reaction energies are controlled by the affinity of the singly reduced TM(IV)═O species to the OH radical (namely, $-BDE_{OH^{\bullet}}$). This is similar to the Bordwell equation[37] for X−H bond dissociation energies (BDEs) used in the community.


dx.doi.org/10.1021/jz3008535 | J. Phys. Chem. Lett. 2012, 3, 2315−2319

Our calculations show that the $OH^{\bullet}$ affinity of TM(IV)=O species of the corresponding TM(V)=O·$H_2O$ complex follows an order of Co(V) > Fe(V) > Mn(V) > Ir(V) > Ru(V) and, hence, has a less endothermic (more exothermic) O−O bond formation process and lower barriers (for details, see Part III in the SI).

Interestingly, the Ru(V)-oxo corrole was found to mediate O−O bond formations with a high barrier (35.1 kcal/mol) and high endothermicity (34.5 kcal/mol). However, we know that polypyridyl−Ru(V)=O systems are currently the workhorses for water oxidation with O−O bond formation rate-limiting steps and with reaction barriers of 19−21 kcal/mol estimated from the experimental rate constants.[16,18] This disparity with Ru(V)−Cor demonstrates that the ligand sphere matters greatly in water oxidation. In the experimentally effective Ru catalysts, the ligands are mostly neutral pyridine/amine-type ligands.[5] However, here, the corrole rings bear −3 charges. This electronic difference can affect the reaction thermochemistry significantly because the high-valent TM=O unit is doubly reduced during the O−O bond formation. It is apparent that a thorough investigation of the ligand effect by experimental and computational means is deemed necessary.

In this work, eight O−O bond formation corrole−TM catalysts were found to have barriers that vary in the following order: Co(V) ≪ Fe(V) < Mn(V) < Ir(V) < Co(IV) < Ru(V) < Ir(IV) < Mn(IV). This order follows the ease of two-electron reduction and the $OH^{\bullet}$ affinity of the TM(IV)=O of the corresponding TM(V)=O·$H_2O$ complex, which together control the reaction thermochemistry. As the study revealed, the Co(V) catalyst, in its Co(IV)−$Cor^{\bullet+}$ $S = 1$ state, is the most effective catalyst among the studied complexes. EER is found to favor the Co(IV)−$Cor^{\bullet+}$ catalyst in its triplet state. Therefore, the experimental result for the cobalt catalysis is derived from a clear physical effect that lowers the energy of the TS. Finally, the charge property of the corrole ligand is implicated to make a difference in the catalytic efficiency of water oxidation.

## ■ ASSOCIATED CONTENT

### Supporting Information

Computational details, four tables of computational results, and Cartesian coordinates of intermediates and transition states. This material is available free of charge via the Internet at http://pubs.acs.org.

## ■ AUTHOR INFORMATION


### Corresponding Author

*E-mail: wenzhenlai@ruc.edu.cn (W.L.); ruicao@ruc.edu.cn (R.C.); chenh@iccas.ac.cn (H.C.).


### Notes

The authors declare no competing financial interest.

## ■ ACKNOWLEDGMENTS

This work is supported by the Fundamental Research Funds for the Central Universities, the Research Funds of Renmin University of China (Program No. 12XNLJ04 to W.L. and No. 12XNLI03 to R.C.), the National Natural Science Foundation of China (No. 21101170 to R.C.), and the Chinese Academy of Sciences (to H.C.). S.S. acknowledges a special grant from Minerva.

## ■ REFERENCES


(1) Dau, H.; Zaharieva, I. Principles, Efficiency, and Blueprint Character of Solar-Energy Conversion in Photosynthetic Water Oxidation. *Acc. Chem. Res.* **2009**, *42*, 1861−1870.

(2) Concepcion, J. J.; Jurss, J. W.; Brennaman, M. K.; Hoertz, P. G.; Patrocinio, A. O. T.; Iha, N. Y. M.; Templeton, J. L.; Meyer, T. J. Making Oxygen with Ruthenium Complexes. *Acc. Chem. Res.* **2009**, *42*, 1954−1965.

(3) Eisenberg, R. Rethinking Water Splitting. *Science* **2009**, *324*, 44−45.

(4) Jiao, F.; Frei, H. Nanostructured Cobalt and Manganese Oxide Clusters as Efficient Water Oxidation Catalysts. *Energy Environ. Sci.* **2010**, *3*, 1018−1027.

(5) Cao, R.; Lai, W. Z.; Du, P. W. Catalytic Water Oxidation at Single Metal Sites. *Energy Environ. Sci.* **2012**, *5*, 8134−8157.

(6) Zong, R.; Thummel, R. P. A New Family of Ru Complexes for Water Oxidation. *J. Am. Chem. Soc.* **2005**, *127*, 12802−12803.

(7) Concepcion, J. J.; Jurss, J. W.; Templeton, J. L.; Meyer, T. J. One Site is Enough. Catalytic Water Oxidation by $[Ru(Tpy)(Bpm)(OH_2)]^{2+}$ and $[Ru(Tpy)(Bpz)(OH_2)]^{2+}$. *J. Am. Chem. Soc.* **2008**, *130*, 16462−16463.

(8) McDaniel, N. D.; Coughlin, F. J.; Tinker, L. L.; Bernhard, S. Cyclometalated Iridium(III) Aquo Complexes: Efficient and Tunable Catalysts for the Homogeneous Oxidation of Water. *J. Am. Chem. Soc.* **2008**, *130*, 210−217.

(9) Gao, Y.; Åkermark, T.; Liu, J. H.; Sun, L. C.; Åkermark, B. Nucleophilic Attack of Hydroxide on a $Mn^{V}$ Oxo Complex: A Model of the O−O Bond Formation in the Oxygen Evolving Complex of Photosystem II. *J. Am. Chem. Soc.* **2009**, *131*, 8726−8727.

(10) Bozoglian, F.; Romain, S.; Ertem, M. Z.; Todorova, T. K.; Sens, C.; Mola, J.; Rodríguez, M.; Romero, I.; Benet-Buchholz, J.; Fontrodona, X.; et al. The Ru-Hbpp Water Oxidation Catalyst. *J. Am. Chem. Soc.* **2009**, *131*, 15176−15187.

(11) Sala, X.; Ertem, M. Z.; Vigara, L.; Todorova, T. K.; Chen, W. Z.; Rocha, R. C.; Aquilante, F.; Cramer, C. J.; Gagliardi, L.; Llobet, A. The Cis-$[Ru^{II}(Bpy)_2(H_2O)_2]^{2+}$ Water-Oxidation Catalyst Revisited. *Angew. Chem., Int. Ed.* **2010**, *49*, 7745−7747.

(12) Blakemore, J. D.; Schley, N. D.; Balcells, D.; Hull, J. F.; Olack, G. W.; Incarvito, C. D.; Eisenstein, O.; Brudvig, G. W.; Crabtree, R. H. Half-Sandwich Iridium Complexes for Homogeneous Water-Oxidation Catalysis. *J. Am. Chem. Soc.* **2010**, *132*, 16017−16029.

(13) Wasylenko, D. J.; Ganesamoorthy, C.; Borau-Garcia, J.; Berlinguette, C. P. Electrochemical Evidence for Catalytic Water Oxidation Mediated by a High-Valent Cobalt Complex. *Chem. Commun.* **2011**, *47*, 4249−4251.

(14) Fillol, J. L.; Codolà, Z.; Garcia-Bosch, I.; Gómez, L.; Pla, J. J.; Costas, M. Efficient Water Oxidation Catalysts Based on Readily Available Iron Coordination Complexes. *Nature Chem.* **2011**, *3*, 807−813.

(15) Romain, S.; Vigara, L.; Llobet, A. Oxygen−Oxygen Bond Formation Pathways Promoted by Ruthenium Complexes. *Acc. Chem. Res.* **2009**, *42*, 1944−1953.

(16) Concepcion, J. J.; Tsai, M.-K.; Muckerman, J. T.; Meyer, T. J. Mechanism of Water Oxidation by Single-Site Ruthenium Complex Catalysts. *J. Am. Chem. Soc.* **2010**, *132*, 1545−1557.

(17) Angeles-Boza, A. M.; Roth, J. P. Oxygen Kinetic Isotope Effects upon Catalytic Water Oxidation by a Monomeric Ruthenium Complex. *Inorg. Chem.* **2012**, *51*, 4722−4729.

(18) Chen, Z. F.; Concepcion, J. J.; Hu, X. Q.; Yang, W. T.; Hoertz, P. G.; Meyer, T. J. Concerted O Atom−Proton Transfer in the O−O Bond Forming Step in Water Oxidation. *Proc. Natl. Acad. Sci. U.S.A.* **2010**, *107*, 7225−7229.

(19) Lin, X. S.; Hu, X. Q.; Concepcion, J. J.; Chen, Z. F.; Liu, S. B.; Meyer, T. J.; Yang, W. T. Theoretical Study of Catalytic Mechanism for Single-Site Water Oxidation Process. *Proc. Natl. Acad. Sci. U.S.A.* **2012**, DOI: 10.1073/pnas.1118344109.

(20) Vilella, L.; Vidossich, P.; Balcells, D.; Lledós, A. Basic Ancillary Ligands Promote O−O Bond Formation in Iridium-Catalyzed Water Oxidation: A DFT Study. *Dalton Trans.* **2011**, *40*, 11241−11247.

(21) Privalov, T.; Åkermark, B.; Sun, L. C. The O−O Bonding in Water Oxidation: The Electronic Structure Portrayal of a Concerted Oxygen Atom−Proton Transfer Pathway. *Chem.—Eur. J.* **2011**, *17*, 8313−8317.
(22) Hughes, T. F.; Friesner, R. A. Systematic Investigation of the Catalytic Cycle of a Single Site Ruthenium Oxygen Evolving Complex Using Density Functional Theory. *J. Phys. Chem. B* **2011**, *115*, 9280−9289.
(23) Vallés-Pardo, J. L.; Guijt, M. C.; Iannuzzi, M.; Joya, K. S.; de Groot, H. J. M.; Buda, F. Ab Initio Molecular Dynamics Study of Water Oxidation Reaction Pathways in Mono-Ru Catalysts. *ChemPhysChem* **2012**, *13*, 140−146.
(24) Chen, Y.; Han, J.; Fang, W.-H. Mechanism of Water Oxidation to Molecular Oxygen with Osmocene as Photocatalyst: A Theoretical Study. *Inorg. Chem.* **2012**, *51*, 4938−4946.
(25) Ertem, M. Z.; Gagliardi, L.; Cramer, C. J. Quantum Chemical Characterization of the Mechanism of an Iron-Based Water Oxidation Catalyst. *Chem. Sci.* **2012**, *3*, 1293−1299.
(26) Vigara, L.; Ertem, M. Z.; Planas, N.; Bozoglian, F.; Leidel, N.; Dau, H.; Haumann, M.; Gagliardi, L.; Cramer, C. J.; Llobet, A. Experimental and Quantum Chemical Characterization of the Water Oxidation Cycle Catalysed by $[Ru^{II}(Damp)(Bpy)(H_2O)]^{2+}$. *Chem. Sci.* **2012**, *3*, 2576−2586.
(27) Dogutan, D. K.; McGuire, R., Jr.; Nocera, D. G. Electocatalytic Water Oxidation by Cobalt(III) Hangman *β*-Octafluoro Corroles. *J. Am. Chem. Soc.* **2011**, *133*, 9178−9180.
(28) Kim, S. H.; Park, H.; Seo, M. S.; Kubo, M.; Ogura, T.; Klajn, J.; Gryko, D. T.; Valentine, J. S.; Nam, W. Reversible O−O Bond Cleavage and Formation between Mn(IV)-Peroxo and Mn(V)-Oxo Corroles. *J. Am. Chem. Soc.* **2010**, *132*, 14030−14032.
(29) Thomas, K. E.; Alemayehu, A. B.; Conradie, J.; Beavers, C. M.; Ghosh, A. The Structural Chemistry of Metallocorroles: Combined X-ray Crystallography and Quantum Chemistry Studies Afford Unique Insights. *Acc. Chem. Res.* **2012**, DOI: 10.1021/ar200292d, and references therein.
(30) Hammond, G. S. A Correlation of Reaction Rates. *J. Am. Chem. Soc.* **1955**, *77*, 334−338.
(31) Bell, R. P. The Theory of Reactions Involving Proton Transfers. *Proc. R. Soc. London, Ser. A* **1936**, *154*, 414−421.
(32) Evans, M. G.; Polanyi, M. Inertia and Driving Force of Chemical Reactions. *Trans. Faraday Soc.* **1938**, *34*, 11−24.
(33) Harvey, J. N.; Poli, R.; Smith, M. K. Understanding the Reactivity of Transition Metal Complexes Involving Multiple Spin States. *Coord. Chem. Rev.* **2003**, *238*−*239*, 347−361.
(34) Janardanan, D.; Usharani, D.; Shaik, S. The Origins of Dramatic Axial Ligand Effects: Closed-Shell $Mn^{V}O$ Complexes Use Exchange-Enhanced Open-Shell States to Mediate Efficient H Abstraction Reactions. *Angew. Chem., Int. Ed.* **2012**, *51*, 4421−4425.
(35) Shaik, S.; Chen, H.; Janardanan, D. Exchange-Enhanced Reactivity in Bond Activation by Metal-Oxo Enzymes and Synthetic Reagents. *Nat. Chem.* **2011**, *3*, 19−27.
(36) Chen, H.; Lai, W. Z.; Shaik, S. Exchange-Enhanced H-Abstraction Reactivity of High-Valent Nonheme Iron(IV)-Oxo from Coupled Cluster and Density Functional Theories. *J. Phys. Chem. Lett.* **2010**, *1*, 1533−1540.
(37) Bordwell, F. G.; Cheng, J.-P. Substituent Effects on the Stabilities of Phenoxyl Radicals and the Acidities of Phenoxyl Radical Cations. *J. Am. Chem. Soc.* **1991**, *113*, 1736−1743.